

Design and Implementation of Two-Stage 3-Level Inverter Grid-Connected for Photovoltaic Applications

Murtadha Jasim Hasan and Fadhil Abbas M. Al-Qrimli
Department of Electrical Engineering, College of Engineering, University of Baghdad,
Baghdad, Iraq
mu.ti.2291@gmail.com

Abstract: In this study proposes a simple, cost effective and efficient system for solar photovoltaic applications. Solar energy is considered as fastest growing renewable energy source after wind energy for electricity generation. Solar energy is a free, clean abundant sun energy considered as inexhaustible source for electricity generation. Solar photovoltaic system is characterized with variable output power due to its operation dependency on solar irradiance and cell temperature. To maximize the energy generation potential of solar PV, research effort is focused on solar cell manufacturing technology to increase its generation efficiency and exploring advancement in power electronic devices for small and large scale deployment. In this study is a single-phase inverter with no transformer for solar PV application. A closed loop DC-DC boost converter that accepts wide input DC voltage assumed to be from 40-60V to produce constant 330V DC voltage is modelled in MATLAB/Simulink. An H-bridge 3-level inverter is used to convert the DC voltage to chopped AC voltage. Then filtered to give pure sinusoidal AC of 230 V RMS. The output voltage of the inverter should have a very low total harmonic distortion within <1% makes the system suitable for local AC load and grid connection.

Key words: Modeling, solar photovoltaic voltage controller, grid-tied inverter, Perturb and Observe (P and O) MPPT, single phase multilevel inverter, SPWM

INTRODUCTION

The prediction of a progressive power method is an accumulation of predictable along with renewable producing sources. The sun oriented is considered on the road to have the maximum possible of force utilization then just before control this force, possible must be located tapped beginning every job of the ground which is accepting sun-powered insolation. The previously mentioned concept has brought winds of change in the conventional recognition of production then load. The concept of the domestic customer organism a load direct control transgressed in the direction of taking place a source because properly, for example, load, the informant being the Rooftop Solar Photovoltaic (RF-SPV) scheme. The spreading stage network mind a marine of drifters then annoyance an operative photovoltaic system ought to take place modelled that nourishes feature power in the direction of the network at the Peak of Common Combination (PCC) by means of the national customer. Production then sends out the purposes. In place of the above-mentioned cause, the job tries in the direction of type an SPV system designed to score the SPV largely comprises of the

subsequent units the photovoltaic array, MMPT boost converter, the inverter, filter then the seclusion transformer. The MPPT holds the energy used for Maximum Power Point (MPP) by attractive criticism of voltage and current starting PV array (Dallago *et al.*, 2015).

MATERIALS AND METHODS

Solar photovoltaic array: An ideal solar PV cell model involves an ideal current source in parallel with an ideal diode as shown in Fig. 1. A photovoltaic array is designed by linking many solar cells in series and parallel fashion. In PV module, series Resistance (R_s) is more predominant and shunt Resistance (R_{sh}) being quite large is assumed to be infinity. As solar insolation increases the open circuit Voltage (V_{oc}) also increases and as temperature increases, the open circuit Voltage (V_{oc}) decreases. The reason being for an increase in temperature, the band gap Energy (E_g) increases resulting in more energy required to traverse the band gap, resulting decrease in efficiency of the PV cell. The simulation work employs model of the panel (150 W) specification of the module are as follows:

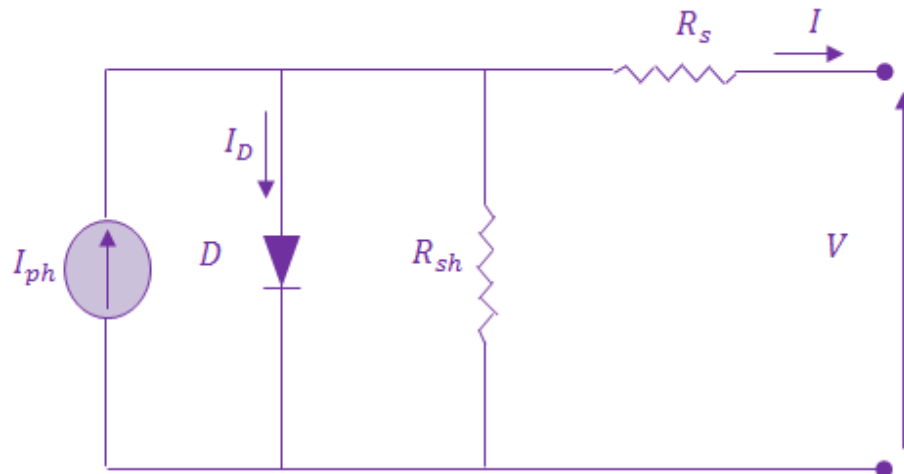


Fig. 1: The equivalent circuit of a PV cell

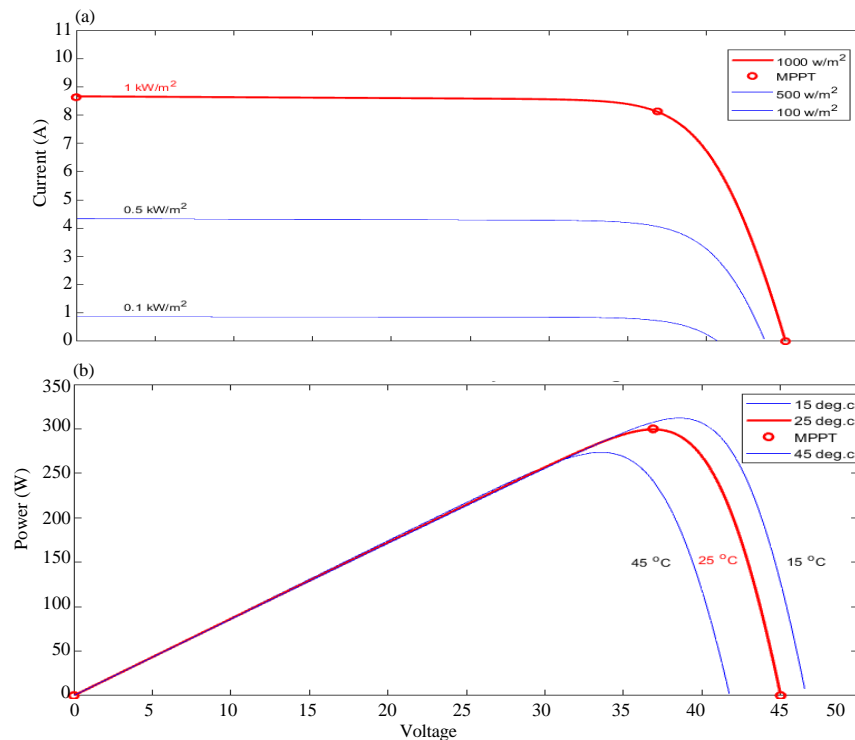


Fig. 2: a) Current-voltage characteristics and b) Power-voltage characteristics of the implemented PV array

- Short circuit current = $I_{sc} = 9.17 \text{ A}$
- Open circuit voltage = $V_{oc} = 21.24 \text{ V}$
- Number of strings in parallel = $N_p = 1$
- Number of series-connected modules per string = $N_s = 2$

The photovoltaic voltage-current characteristic is non-linear during natural operation the same as shown in Fig. 2. The power production intended for a certain

radiance along with temperatures starting. The a maximum point increases through an increase inside the cell where output current starting the call the direct taking place, so, the V-I characteristics giving the maximum power are called the maximum power point designed for the particular Irradiance in addition to temperature. This maximum power point tracking algorithm (Dallago *et al.*, 2015) which gives the voltage by the side of which maximum power is given by the PV cell.

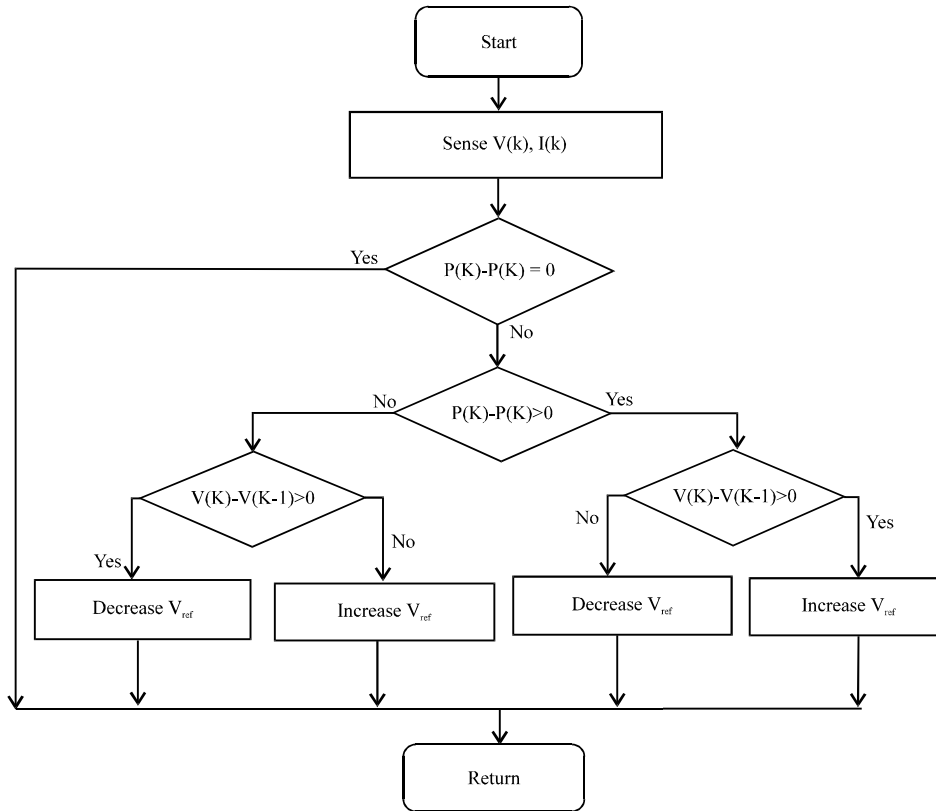


Fig. 3: Flowchart of the perturb and observe algorithm

Maximum power point tracking: The MPPT is a methodology taken after towards gathering the mainly created power on or after certain sources be partial to PV systems then storm turbine (Hua and Shen, 1998). During this investigation, this the calling was defended by a microcontroller-based DC towards the DC converter with the aim of optimizes the equivalent of the solar array (PV panels) as well as the load. Easily it is an algorithm encouraged by the principles of the voltage and current of the panel by the side of every one moment (Zhang *et al.*, 2011).

The panel emerges next to daytime. This characteristically gives concerning a 15% increase in power during Winter in addition to up to a 35% increase during Summer. This is common in locales contain short time but inside the Middle East Region by the side of the majority time inside the year has a long day then using a sun tracker choice not create a real change inside the production of the panel (Wang and Lu, 2013; Bazaryari *et al.*, 2014). In place of our work we contain utilized the Perturb and Observe (P and O) method in addition called “Hill-Climbing” is the majority generally, utilized method designed for MPPT because of its plainness in addition to efficiency (Femia *et al.*, 2005; Atallah *et al.*, 2014). The P and O is used in this research for instance MPPT method. The flowchart of the P and O algorithm is shown in Fig. 3.

MPPT boost converter: Around are plentiful converter topologies obtainable in place of MPPT converter actualized the same as seen during the creative writing (Schaefer and Stauth, 2014; Hua and Shen, 1998; (Bazaryari *et al.*, 2014) designed for our research we include determined leading boost converter topology. The PV cell is a current source, consequently, the essentiality deformation inside maintenance a constant voltage summarizes crossways the load intended for maximum taking out of power intended for changing insolation levels in addition to temperature.

The input capacitor is required on the way to stabilize the input voltage appropriate towards the peak current obligation of switching power source. The input capacitor is chosen at this juncture is: $C_1 = 300 \mu F$. The choice of the inductor is of superior significance seeing that inductor lying on the enter boundary of the converter stores energy in addition to giving incessant input current waveform. Evaluated beginning the formula:

$$L_{min} = \frac{V_{in} \times (V_{out} - V_{in})}{\Delta I_L \times f_s \times V_{out}} \quad (1)$$

L_{min} is the minimum value inductor necessary intended for boost process with no saturation of the central part of the

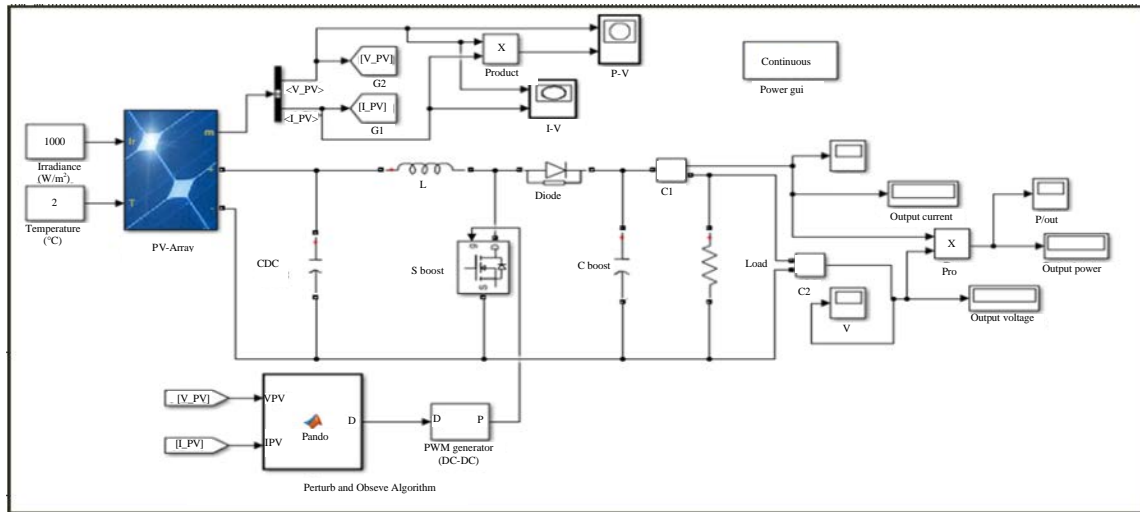


Fig. 4: Design boost converter and MPPT control

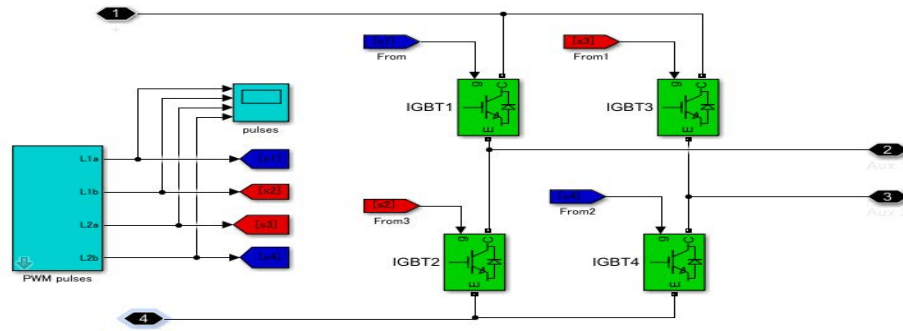


Fig. 5: Grid-tied inverter and multilevel controller

inductor. $V_{in} = 40\text{--}60\text{ V}$, input voltage beginning solar PV $V_{OUT} = 330\text{ V}$, the output voltage of the MPPT boost converter, i.e., the voltage comparing to maximum power point. The $f_s = 20\text{ kHz}$, switching frequency of the MOSFET, S_{Boost} shown in Fig. 4.

$$\Delta I_L = (0.2 - 0.4) \times I_{out(max)} \times \frac{V_{out}}{V_{in}} \quad (2)$$

This current ripple is not accepted, previous is like this approximation of 20% towards 40%. $I_{out(max)} = 0.91\text{ A}$ is the maximum output current of this MPPT converter $\Delta I_L = 2.86\text{ A}$ is the current ripple of the inductor [from Eq. 2]. $L_{min} = 1.43\text{ mH}$ is assessed from Eq. 1 and 2. The inductor chosen intended for this converter is $L_1 = 1.286\text{ mH}$, so, the output capacitor is chosen towards minimizing the output ripple voltage is assessed by the formula: MOSFET, S_{Boost} shown in Fig. 4.

$$C_{out(min)} = \frac{I_{OUT(max)} \times D}{\Delta V_{OUT} \times f_s} \quad (3)$$

where, the D = Duty cycle of the converter which is accepted towards being located, 25% with acknowledging to 40 V organism input and 330 V for the instance output of the MPPT converter. $\Delta V_{out} = 3.3\text{ V}$, voltage ripple is accepted $C_{OUT(MIN)} = 120\mu\text{F}$ is calculated from Eq. 3. We contain occupied $C_2 = 120\mu\text{F}$ for our simulation purpose intended to improved voltage waveform.

Grid Tied Inverter (GTI): Grid-tied inverter theatres the significant position in the solar photovoltaic grid-tied power technique. The job of a GTI is double. Single creature of changing over DC power beginning SPV to AC power which is in the direction of being located given to network then the previous organism to realize, so as to in a shape that the photovoltaic panel otherwise array is spared as of response of network connected. Readily available are frequent topologies planned in creative writing (Atallah *et al.*, 2014). Which utilizes a extensive breadth of semiconductor switches. Intended for our job we contain conceived a single phase H-Bridge inverter by means of IGBT existence our high-frequency switch as revealed in Fig. 5.

After the platform boosting, the DC power is connected to the inverter to modernize towards AC power. In that case, this favorably harmonic response is accepted through a filter which causes a damaging effect on the harmonics to obtain a suitable sinusoidal response. An awfully low Total Harmonics Distortion (THD) is achievable by appropriate determination of filter.

Designed for our modelling, we choose the Sinusoidal Pulse Width Modulation (SPWM) for instance, our gating technique to IGBT then an LCL filter configuration, causing the gating pulse to be constrained on a gate of IGBT of H-Bridge. The sacking arrangement is such that S1 and S4 Fig. 5 changes their switching situation consistently then the opposite switching situation is conventional by S2 and S3 simultaneously. Thereby generous an in close proximity sinusoidal ventured output which is filtered towards reducing THD, so as to can be established by the network standard (Zhang *et al.*, 2011).

Circuit parameters for the simulation and hardware implementation;

List of parameters with specifications used for the design;

PV array:

- Model: solartech energy ASC 6P-36-150
- Short circuit current = $I_{sc} = 9.17$
- Open circuit voltage = $V_{oc} = 21.24$
- Number of cells per module = 36
- Number of strings in parallel = $N_p = 1$
- Number of series-connected modules per string = $N_s = 2$

MPPT converter:

- $C1 = 120 \mu F$
- $L1 = 1 mH$
- $C2 = 120 \mu F * 4$

Inverter:

- Sinusoidal PWM switching frequency 20 kHz
- Inverter output voltage = 330 V(peak)
- 230 V (RMS), THD = 2.92%

T-or LCL filter:

- $L2 = 14mH$
- $C3 = 2\mu F$
- $L3 = 14Mh$

Power grid:

- $V_{GRID(RMS)} = 230 V$
- Grid frequency = 50 Hz

Filter modeling: Filters are utilized just before keeping in check the harmonic satisfied during the current waveform of a scheme like this progresses the source voltage waveform (Wu *et al.*, 2014). In our occupation, we contain utilized streak filters as it reduces the harmonic satisfy during currently fashioned by the high-frequency switching process in PWM inverters, the line filters L and T-filter is principally utilized.

L-filter: L-filters are first order filters having a constriction 20 dB/decade in excess of an extensive range of frequency. Intended for very high switching frequency PWM inverter it causes good quality attenuation.

T or LCL filter: The T-filter are comparatively improved than L-filter for constriction of switching harmonics for PWM inverter In addition, other profit of using the T-filter creature:

- Current distortion is low down then the generation of reactive power
- Attenuation of -60 dB/decade designed for frequencies acceptably more than the resonant frequency

For a provide harmonic decrease, the lower switching frequency can take place utilized T-filter in addition forces the improvement of low THD stable at the low switching frequency than by a smaller amount storage space of energy. Hence, we chose T-filters designed for our occupation. In addition to our choice filter, the meaning is: With a THD = 4.31%. At the moment the AC power following taking into consideration the filter drop meets the acceptable network THD standards (Nguyen *et al.*, 2014) which is fewer than 5% THD in addition to fulfils the voltage level regular of a creature more than network voltage with the intention of can take place encouraged to the power network.

RESULTS AND DISCUSSION

Simulation modul and simulation results: The projected system was actualized on MATLAB R2017a platform in addition to the results are discussed in this subdivision. The aggregate operational Simulink circuit diagram is made known in Fig. 6-8. The irradiance in addition to temperature were given in the direction of PV array utilizing single builder group of buildings in Simulink, the levels of irradiance in addition to signal builder building block in Simulink. In this simulation, the power network is arranged such, so as to the voltage of the network changes from 230-220 V (RMS), respectively, the location

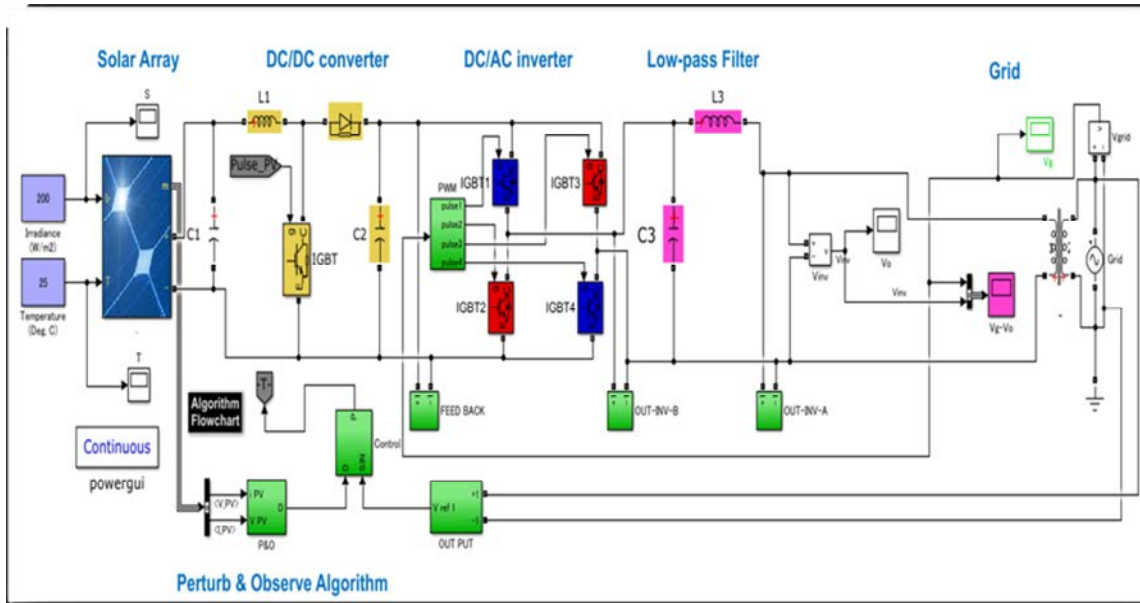


Fig. 6: The simulation diagram single phase, h-bridge, 3-level inverter using MATLAB

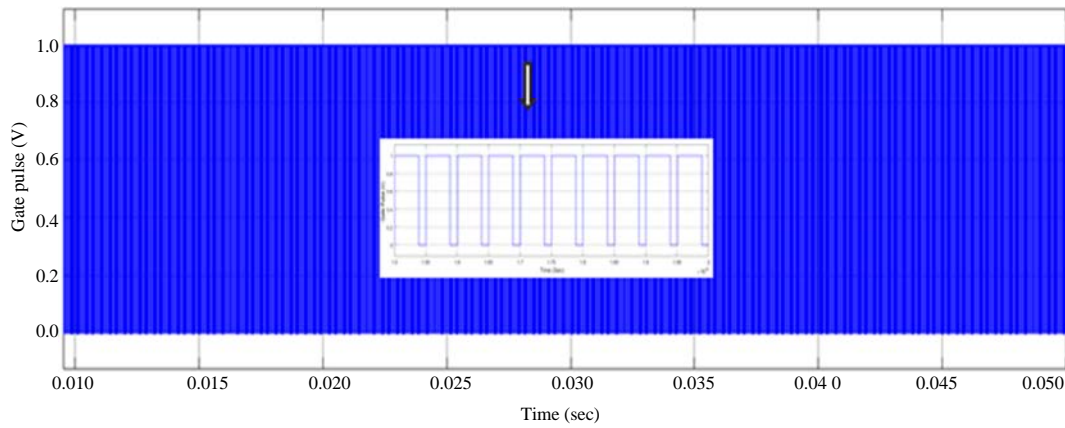


Fig. 7: Pulse of the boost converter

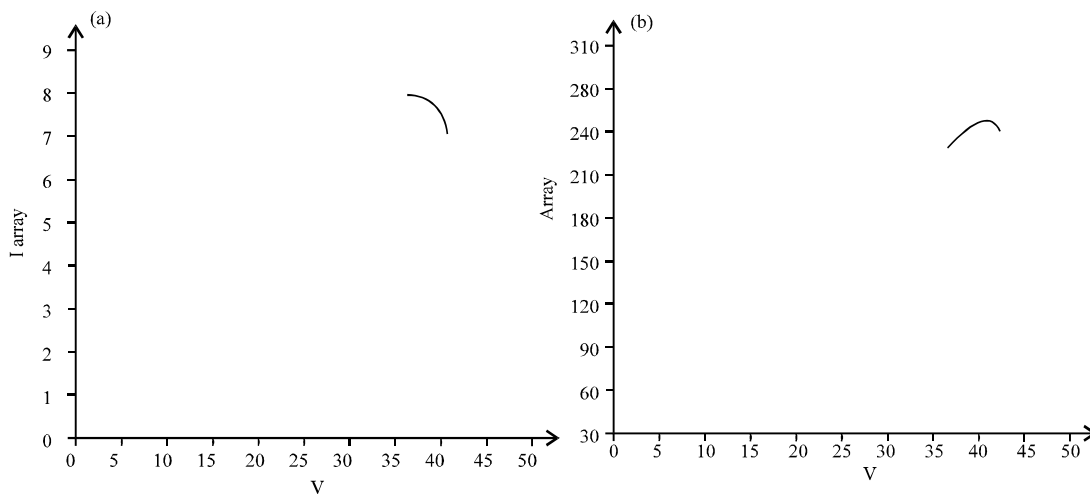


Fig. 8: a) I-V characteristics of the MPPT control and b) P-V characteristics of the MPPT control

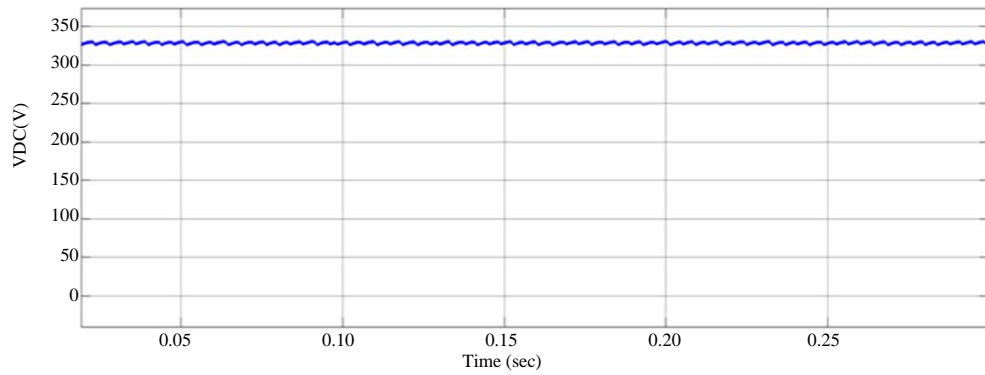


Fig. 9: Voltage of boost converter by using MPPT

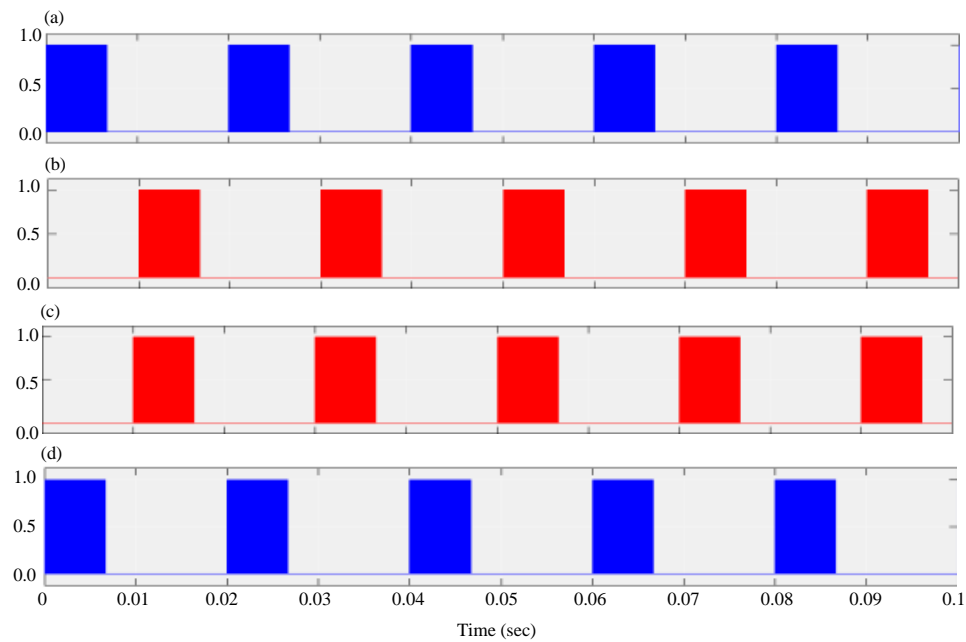


Fig. 10: a-d) Three-level Sinusoidal Pulse Width Modulation (SPWM) gate of the inverter

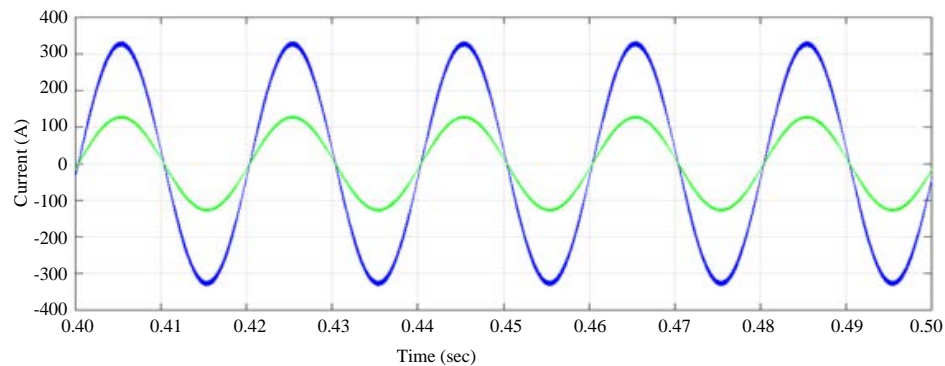


Fig. 11: Voltage and current*(100) profiles of inverter after the filter

from the network such as tapped by the PLL block changes towards generating closed-loop control signals designed for the inverter, an active exhibitions estimation

has been surveyed on the designed controllers. The voltage profiles of the, MPPT stage featuring in Fig. 9-11. Keeping up the imperative of the inverter output voltage

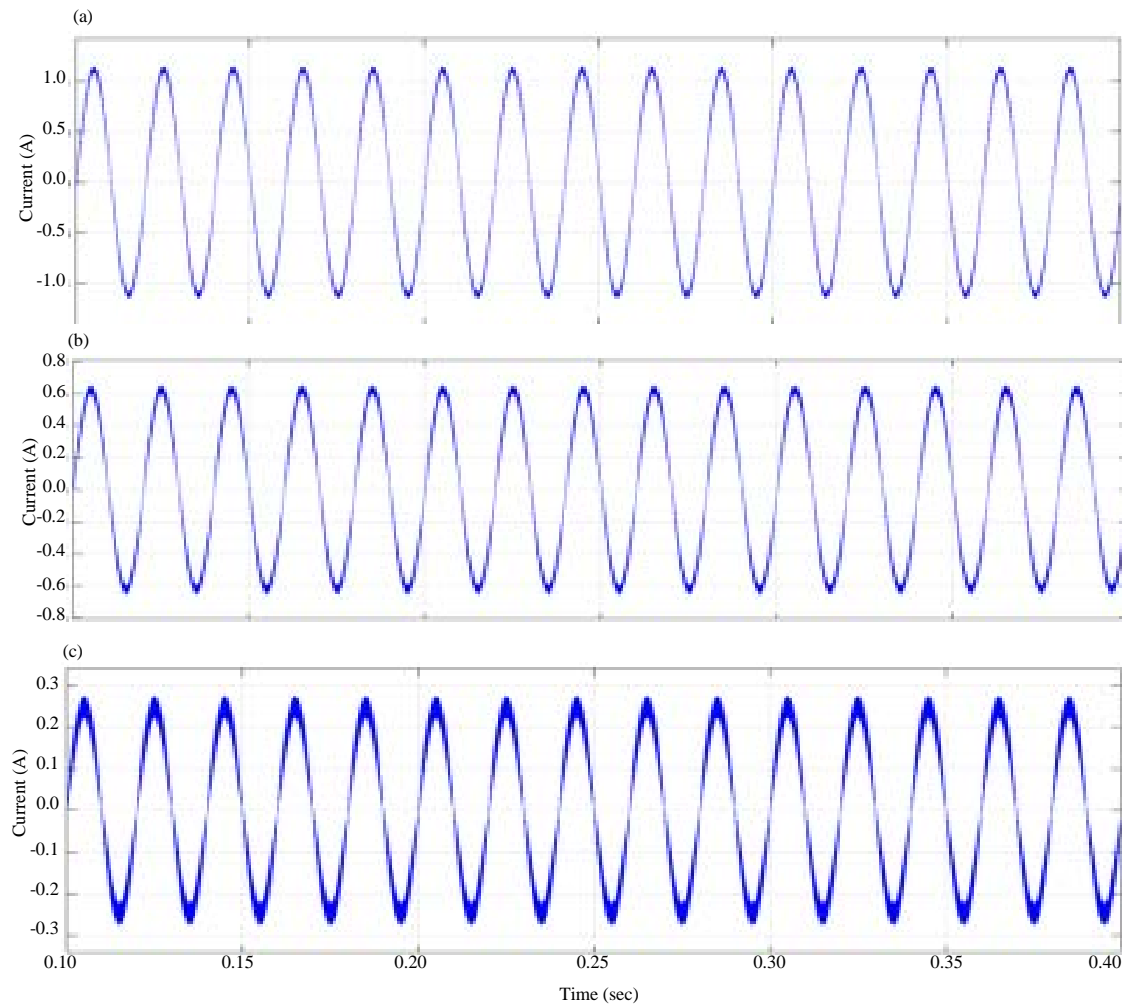


Fig. 12: a) $P_{in} = 250 \text{ W}$, $THD = 2.921\%$; b) $P_{in} = 150 \text{ W}$, $THD = 4.08\%$ and c) $P_{in} = 50 \text{ W}$, $THD = 6.344\%$

Table 1: Different simulation results with different sunlight radiation values for the single-phase H-bridge 3-level Inverter

$S \text{ (W/m}^2\text{)}$	$P_n \text{ (W)}$	THD (%)	P.F	$I_n \text{ rms sec (A)}$	$P_n \text{ (W)}$	$\eta \text{ (\%)}$
1000	250	2.912	0.999100	0.9454	217.442	86.9768
921	232	2.998	0.998900	0.9010	207.230	89.3230
810	217	3.082	0.998600	0.8620	198.260	91.3640
716	205	3.185	0.998500	0.8036	184.828	90.1600
632	183	3.269	0.998360	0.7230	166.290	90.0300
524	161.2	3.591	0.997800	0.6110	140.530	87.1770
406	146.1	4.128	0.993900	0.5412	124.476	85.2570
351	123	4.762	0.989800	0.4605	105.800	86.0160
242	97	5.315	0.986869	0.3561	81.9030	84.4360
103	48	5.972	0.985980	0.1698	39.1540	81.7740

is more than the network voltage the output of the inverter after the filters creature 330 V (peak). The THD is 2.92% as the network voltage changes following filtering the sinusoidal summarize AC power are connected headed for the power network by means of an isolation transformer. The output voltage waveform starting inverter before the filter.

Different values of the output current fed to grid for different sunlight radiations and for 25°C temperature is shows in Fig. 12 and Table 1.

Hardware implementation and experimental results

The design of the boost converter by using proteus: Figure 13 shows the boost converter design.

Control circuit implementation: Figure 14 shows the control schematic diagram of the H-bridge 3-level inverter.

DC power supply: Figure 15 shows the regulators connection circuits.

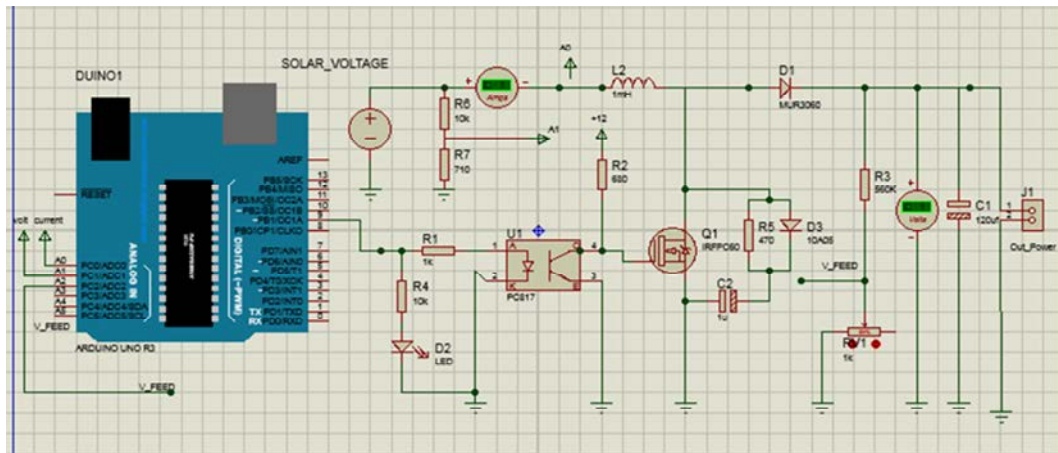


Fig. 13: Boost converter design

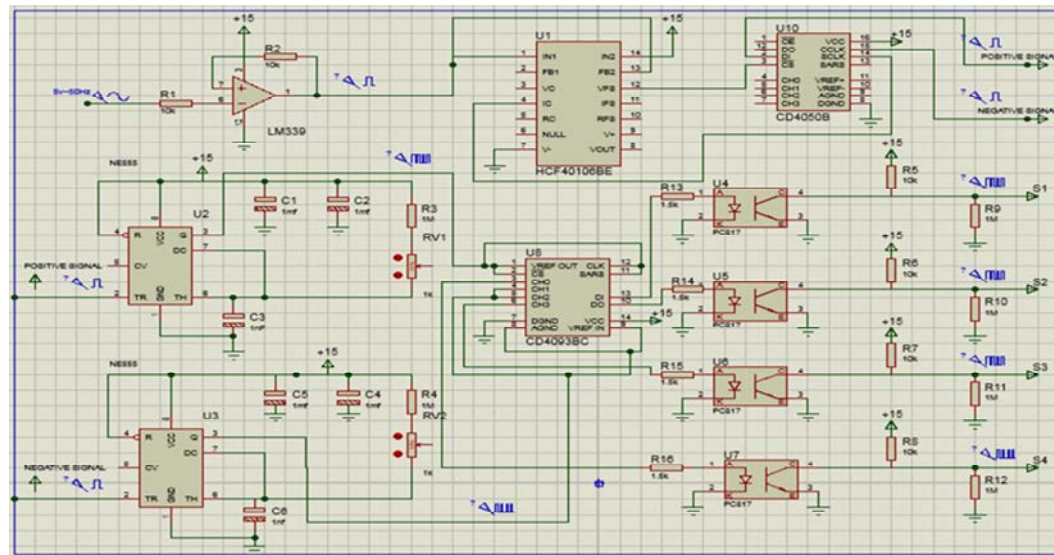


Fig. 14: Control schematic diagram of the H-bridge 3-level inverter

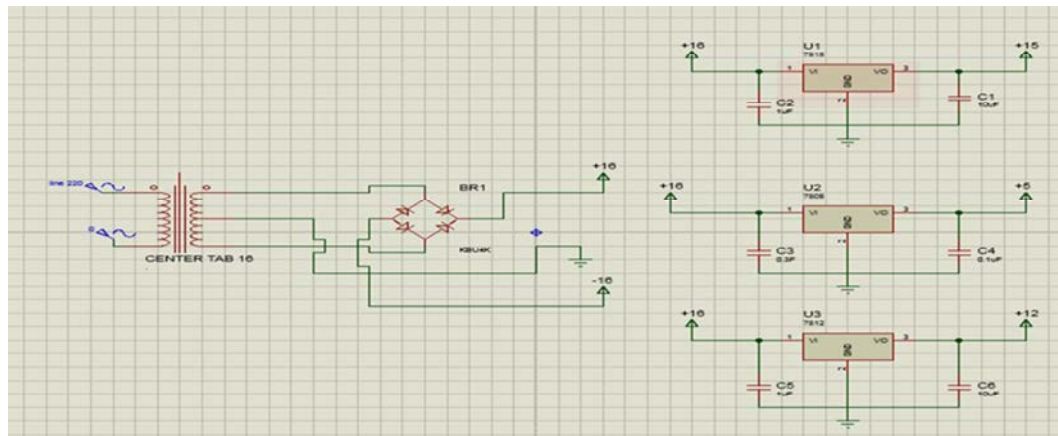


Fig. 15: Regulators connection circuits

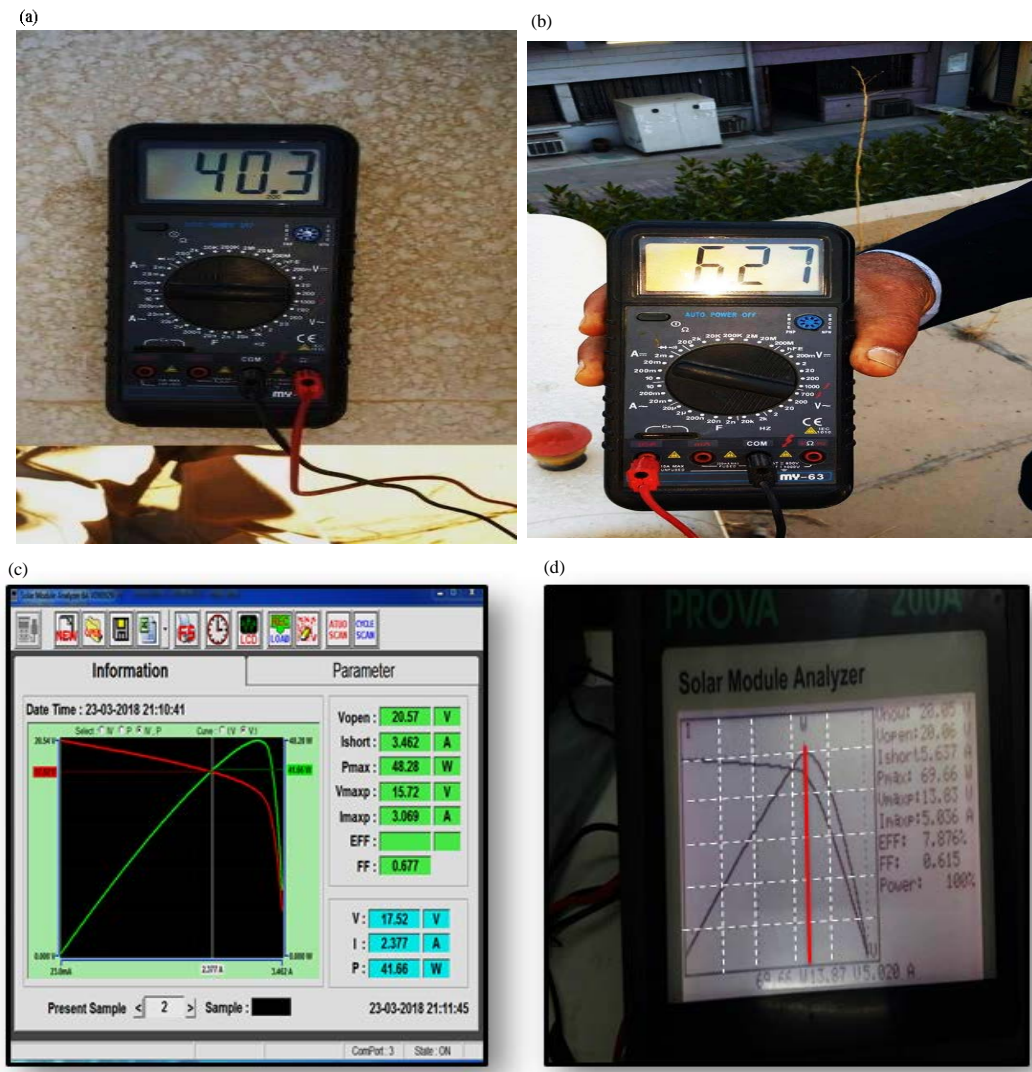


Fig. 16: a-d) The characteristics between the voltage and current for the output PV

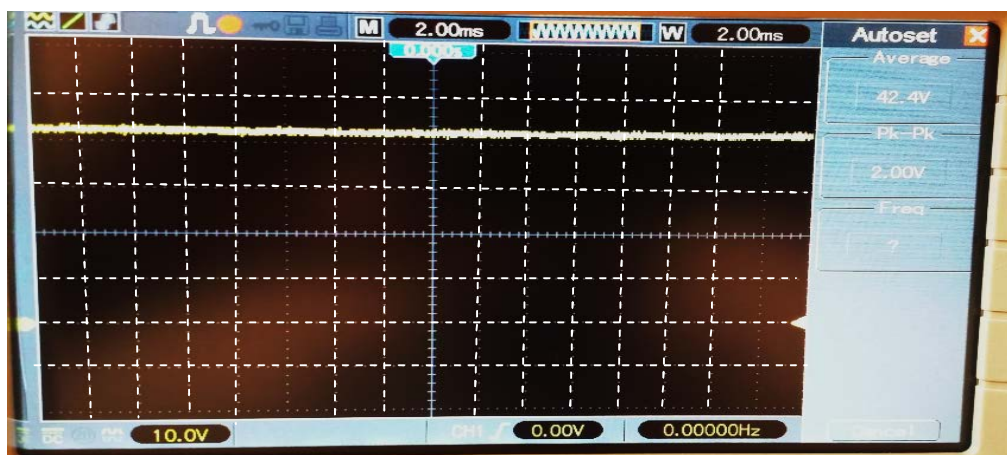


Fig. 17: Output voltage for the PV array

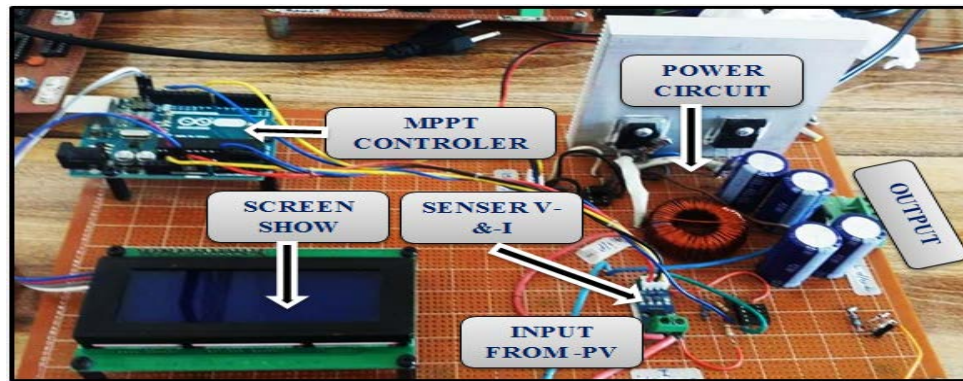


Fig. 18: The power circuit and MPPT control circuit

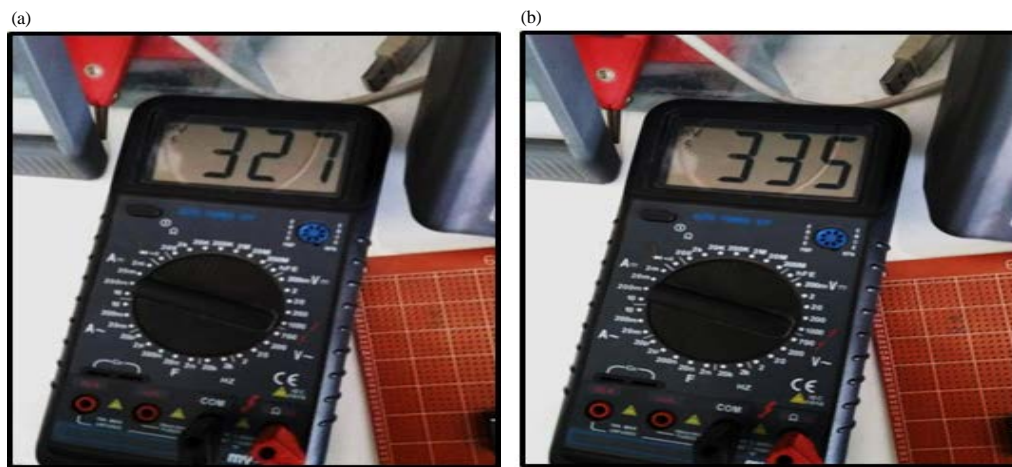


Fig. 19: a, b) The output for the boost converter

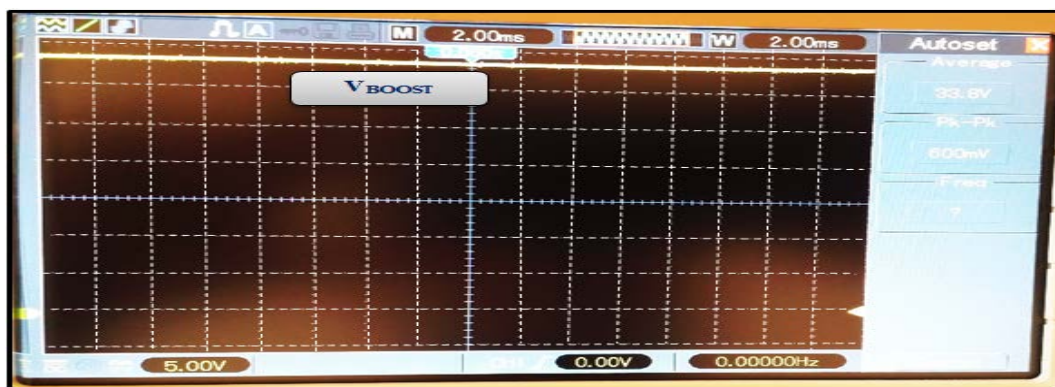


Fig. 20: The wave for the output boost converter

PV array: The voltage and current output for the PV array at when the sunlight radiation is 868 W/m^2 (Fig. 16-20).

Boost converter: The gate pulses sequence for the main switch for boost converter and shows the

gatepulses for both S_1 - S_4 switches for inverter is shown in Fig. 21-25 and Table 2. The experimental results for the current injected to the grid for different values of S and different values of input power with Temperature of $T = 25^\circ\text{C}$ other factors are also shown like the efficiency

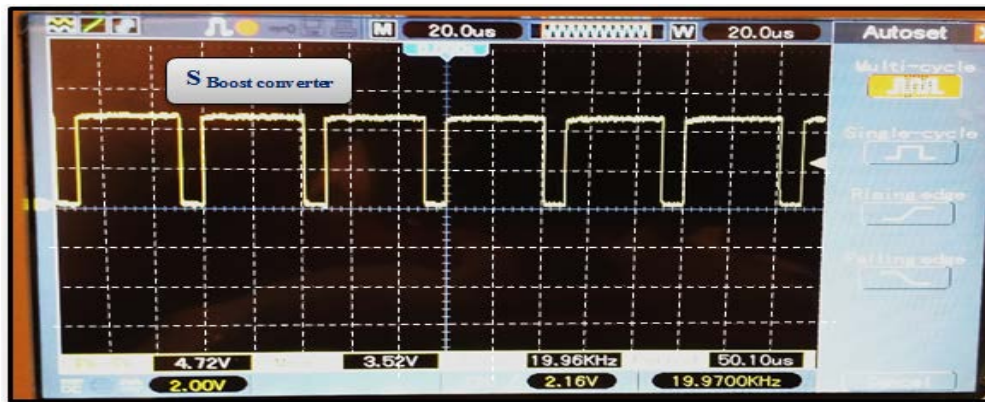


Fig. 21: The pulse for the switch power circuit

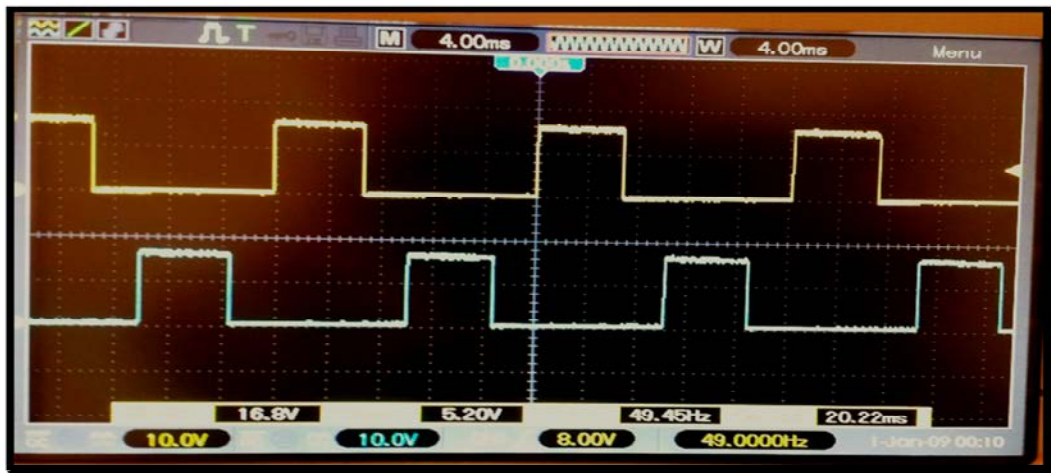


Fig. 22: The pulse for the switch S_1 - S_4 for the inverter

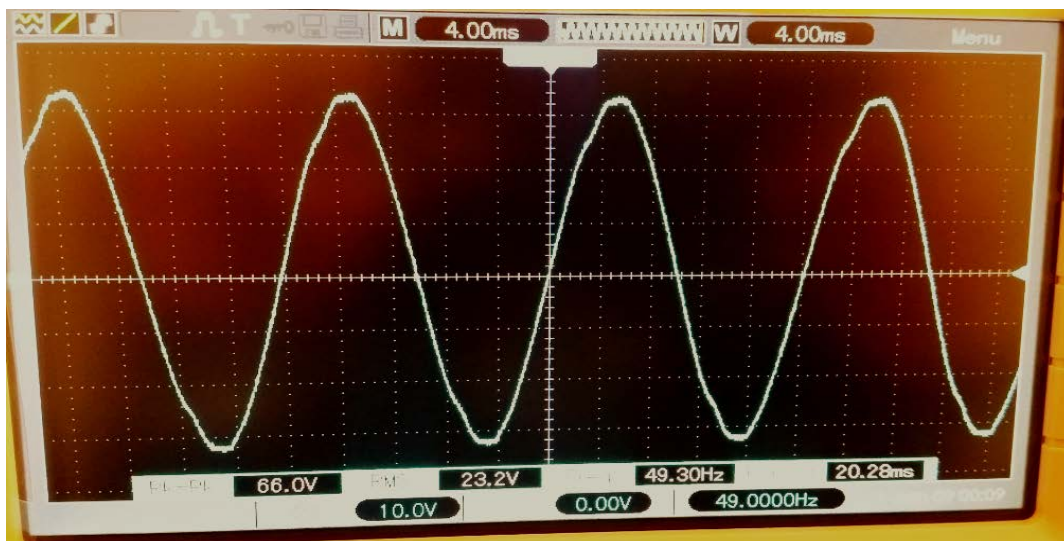


Fig. 23: Voltage output profiles of the inverter

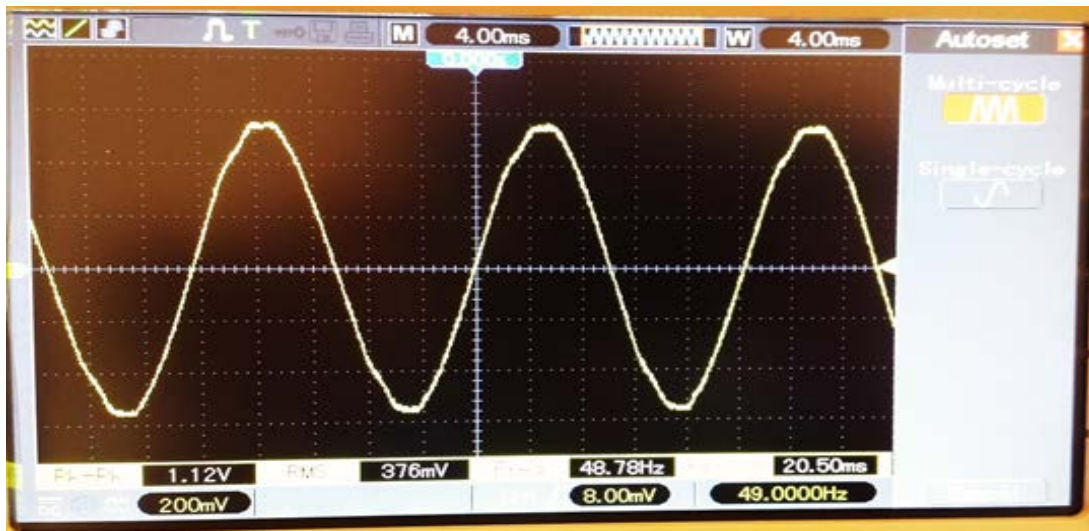


Fig. 24: Current output profiles of the inverter by using load 120 W

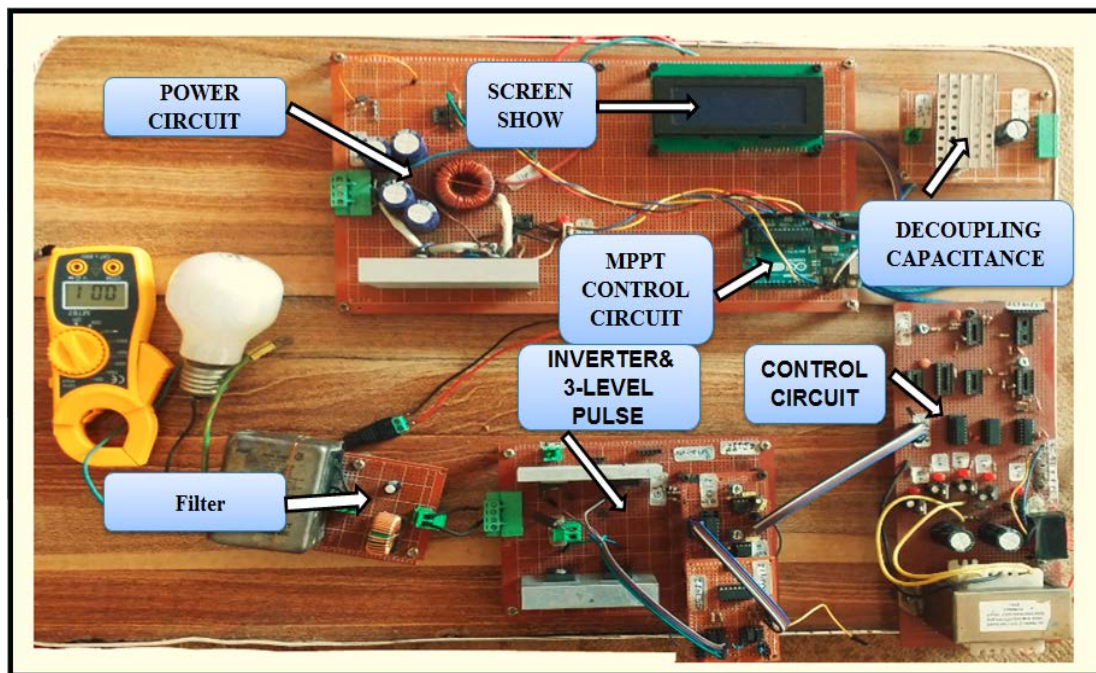


Fig. 25: System setup, power circuit and control circuits

Table 2: Different experimental results for different values of S

S (W/m ²)	P _m (W)	THD (%)	P.F	I _o rm sec (A)	P _o (W)	η (%)
840	232	3.2820	0.992160	0.8890	204.470	88.133
723	212	3.1850	0.991500	0.7930	182.828	86.033
632	186	3.1210	0.997360	0.7530	172.290	90.030
535	165.2	3.6300	0.997600	0.6110	143.530	86.882
406	146.1	4.6860	0.991900	0.5508	124.476	85.852
312.6	126	4.8690	0.980800	0.4605	105.800	83.397
258	98.56	5.4020	0.988869	0.3761	83.8130	85.037
113	44.843	5.9812	0.975980	0.1598	36.1540	80.623

(η) and THD. The results show good performance for the single-phase H-bridge 3-level inverter for injecting

alternating current to the national grid with high efficiency and low total harmonic distortion is shows in Table 2.

CONCLUSION

Fasten indicating the MPP beginning the VI curves contain been tended to by a variety of algorithms, shown of which for the most part common are the Perturb and Observe (P and O) (Elgendy *et al.*, 2012). Then the Incremental Conductance (INNCND) (Kish *et al.*, 2012) quite a lot of adjustments of these calculations contain been projected in current a long time which brightly calculates pace dimension, tracks MPP inside antenna less procedure, put in progressive cleverly fuzzy then neural method to exactly recognize the MPP (Sher *et al.*, 2015; Kollimalla and Mishra, 2014).

REFERENCES

- Atallah, A.M., A.Y. Abdelaziz and R.S. Jumaah, 2014. Implementation of perturb and observe MPPT of PV system with direct control method using buck and buck-boost converters. *Emerging Trends Electr. Electron. Instrum. Eng. Intl. J.*, 1: 31-44.
- Bazyari, S., R. Keypour, S. Farhangi, A. Ghaedi and K. Bazyari, 2014. A study on the effects of solar tracking systems on the performance of photovoltaic power plants. *J. Power Energy Eng.*, 2: 718-728.
- Dallago, E., A. Liberale, D. Miotti and G. Venchi, 2015. Direct MPPT algorithm for PV sources with only voltage measurements. *IEEE. Trans. Power Electron.*, 30: 6742-6750.
- Elgendy, M.A., B. Zahawi and D.J. Atkinson, 2012. Assessment of perturb and observe MPPT algorithm implementation techniques for PV pumping applications. *IEEE. Trans. Sustainable Energy*, 3: 21-33.
- Femia, N., G. Petrone, G. Spagnuolo and M. Vitelli, 2005. Optimization of perturb and observe maximum power point tracking method. *IEEE Trans. Power Electr.*, 20: 963-973.
- Hua, C. and C. Shen, 1998. Study of maximum power tracking techniques and control of DC/DC converters for photovoltaic power system. *Proceedings of the 29th Annual IEEE Conference Power Electronics Specialists (Cat. No.98CH36196)(PESC 98 Record)* Vol. 1, May 22, 1998, IEEE, Fukuoka, Japan, ISBN:0-7803-4489-8, pp: 86-93.
- Kish, G.J., J.J. Lee and P.W. Lehn, 2012. Modelling and control of photovoltaic panels utilising the incremental conductance method for maximum power point tracking. *IET. Renewable Power Gener.*, 6: 259-266.
- Kollimalla, S.K. and M.K. Mishra, 2014. A novel adaptive P&O MPPT algorithm considering sudden changes in the irradiance. *IEEE. Trans. Energy Convers.*, 29: 602-610.
- Nguyen, L.V., H.D. Tran and T.T. Johnson, 2014. Virtual prototyping for distributed control of a fault-tolerant modular multilevel inverter for photovoltaics. *IEEE. Trans. Energy Convers.*, 29: 841-850.
- Schaefer, C. and J.T. Stauth, 2014. Multilevel power point tracking for partial power processing photovoltaic converters. *IEEE. J. Emerging Sel. Top. Power Electron.*, 2: 859-869.
- Sher, H.A., A.F. Murtaza, A. Noman, K.E. Addoweesh and K. Al-Haddad *et al.*, 2015. A new sensorless hybrid MPPT algorithm based on fractional short-circuit current measurement and P&O MPPT. *IEEE. Trans. Sustainable Energy*, 6: 1426-1434.
- Wang, J.M. and C.L. Lu, 2013. Design and implementation of a sun tracker with a dual-axis single motor for an optical sensor-based photovoltaic system. *Sens.*, 13: 3157-3168.
- Wu, W., Y. Sun, M. Huang, X. Wang and H. Wang *et al.*, 2014. A robust passive damping method for LLCL-filter-based grid-tied inverters to minimize the effect of grid harmonic voltages. *IEEE. Trans. Power Electron.*, 29: 3279-3289.
- Zhang, L., W.G. Hurley and W.H. Wolfe, 2011. A new approach to achieve maximum power point tracking for PV system with a variable inductor. *IEEE. Trans. Electron.*, 26: 1031-1037.